

# ParFormer: Vision Transformer Baseline with Parallel Local Global Token Mixer and Convolution Attention Patch Embedding

Novendra Setyawan<sup>1,2</sup>, Ghufron Wahyu Kurniawan<sup>3</sup>, Chi-Chia Sun<sup>4</sup>, Jun-Wei Hsieh<sup>5</sup>, Hui-Kai Su<sup>6</sup>, and Wen-Kai Kuo<sup>7</sup>

<sup>1</sup> Department of Electro-Optical Engineering, National Formosa University, Taiwan

<sup>2</sup> Department of Electrical Engineering, University of Muhammadiyah Malang, Indonesia

`novendra@umm.ac.id, d1277102@nfu.edu.tw`

<sup>3</sup> Department of Electrical Engineering, National Formosa University, Taiwan

`11165151@nfu.edu.tw`

<sup>4</sup> Department of Electrical Engineering, National Taipei University, Taipei, Taiwan

`chichiasun@gm.ntpu.edu.tw`

<sup>5</sup> College of Artificial Intelligence and Green Energy, National Yang Ming Chiao

Tung University, Taiwan

`jwhsieh@nycu.edu.tw`

<sup>6</sup> Department of Electrical Engineering, National Formosa University, Taiwan

`hksu@nfu.edu.tw`

<sup>7</sup> Department of Electro-Optical Engineering, National Formosa University, Taiwan

`wkkuo@nfu.edu.tw`

**Abstract.** Transformer designs have shown superior performance compared to CNN models in several computer vision tasks. The prevailing assumption is that their skill is mostly attributed to architectural designs that utilize attention-based token mixing. Self-attention in transformer networks enables the integration of visual relationships across great distances, leading to a wide, possibly global receptive field. Conversely, a convolution token mixer can efficiently capture image information with little dependencies. This work presents ParFormer as an enhanced transformer architecture that allows the incorporation of different token mixers into a single stage, hence improving feature extraction capabilities. Integrating both local and global data allows for precise representation of short- and long-range spatial relationships without the need for computationally intensive methods such as shifting windows. Along with the parallel token mixer encoder, We offer the Convolutional Attention Patch Embedding (CAPE) as an enhancement of standard patch embedding to improve token mixer extraction with a convolutional attention module. Our comprehensive evaluation demonstrates that our ParFormer outperforms CNN-based and state-of-the-art transformer-based architectures in image classification and several complex tasks such as object recognition. The proposed CAPE has been demonstrated to benefit the overall MetaFormer architecture, even while utilizing the Identity Mapping Token Mixer, resulting in a 0.5% increase in accuracy. The ParFormer models outperformed ConvNeXt and

Swin Transformer for the pure convolution and transformer model in accuracy. Furthermore, our model surpasses the current leading hybrid transformer by reaching competitive Top-1 scores in the ImageNet-1K classification test. Specifically, our model variants with 11M, 23M, and 34M parameters achieve scores of 80.4%, 82.1%, and 83.1%, respectively. Code: <https://github.com/novendrastym/ParFormer-CAPE-2024>

**Keywords:** Transformer · Neural Networks · Image Classification · Object Detection · Parallel Token Mixer

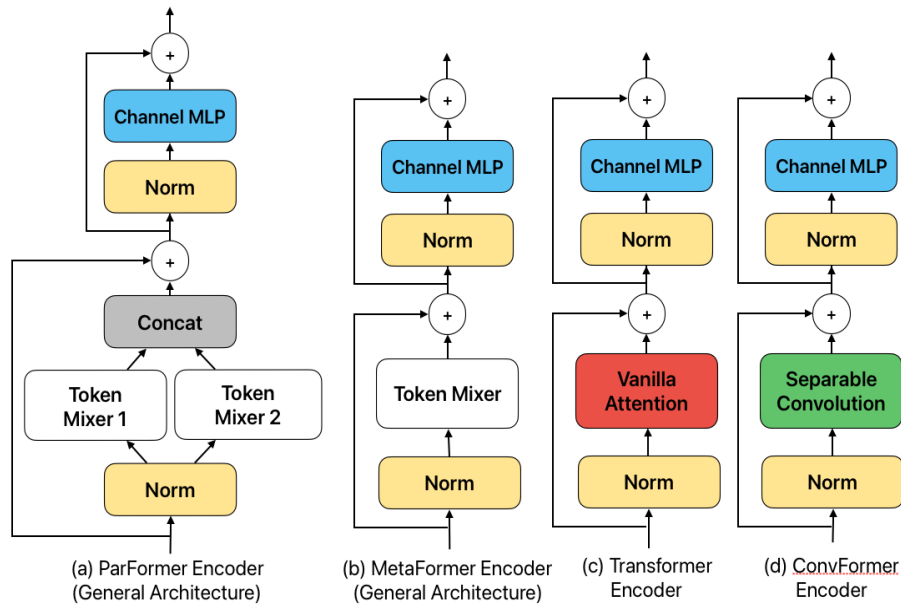


**Fig. 1: Comparisons among different transformer architectures.** (a) Parformer; (b) Metaformer; (c) Transformer; (d) ConvFormer;

## 1 Introduction

In recent years, Transformers have garnered significant attention and demonstrated an exhibited remarkable achievement in computer vision [2, 5, 11]. There has been a notable development in the field of vision transformers, particularly after the introduction of the Vision Transformer (ViT) [15]. The ViT model utilizes pure Transformers for image classification tasks. Subsequently, several models have been developed to improve performance and achieve promising outcomes in various downstream vision transformer tests [38, 40, 50, 56]. These tests encompass a range of applications such as image classification, object detection, and segmentation.

Since the inception of the initial ViT model, several claim that its effectiveness can be attributed to the phenomenon of attention mechanisms [41]. Several versions of attention mechanisms have been proposed in numerous studies [9,22,28,45], stemming from this particular assumption. Furthermore, in order to enhance the efficacy of attention-based transformers, various studies have explored the parallelism of diverse token mixers [6, 16, 26, 51]. In this particular study, the researchers have employed a combination of two distinct attention mechanisms in order to augment the process of feature extraction, hence enhancing the model’s ability to capture both global and local dependencies. However, multiple research studies have demonstrated that the performance of transformers is contingent upon their architectural design, commonly referred to as MetaFormer [53,54]. This studies have shown evidence that even in the absence of operators such as identity in IdentityFormer or non-parametric operations like pooling in PoolFormer, the model still achieves state-of-the-art performance when compared to transformers with learnable operation token mixers.

In addition to the Attention Module, numerous studies have been conducted to enhance the Transformer architecture. One approach involves using overlapped patch embedding to improve local continuity, as opposed to the hard patching used in the original Transformer [46, 50]. Furthermore, employing the "patchify" approach or utilizing Patch Embedding as a down-sample layer can enhance the performance in ConvNeXt [48]. The model employing a 4-stages framework exhibits more advancement compared to the isotropic style architecture, even when considering similar parameters and FLOPs [55]. It has been demonstrated that the down-sampling layer is essential when reducing the spatial resolution and projecting the feature into the higher channel.

Based on the hypotheses presented in the previous cumulative research, it is observed that the transformer architecture, consisting of two residuals block (token mixer block and MLP) shows in Figure 1(b), plays a crucial role in achieving competitive performance when compared to the specific token mixer. Furthermore, the implementation of a token mixer block with employing the combination of local and and global extractor can effectively decrease the overall computational workload without compromising its competitive performance. Hence, this study introduces the Parallel Transformer architecture, referred to as "ParFormer," as a comprehensive transformer framework that explore the transformer structure by enables the integration of two separate token mixers (such as local and global feature extractor), as depicted in Figure 1(a). The architectural progress in the field of architecture has played a significant role in the evolution of vision model architectures, which have a striking resemblance to Convolution Neural Networks or Pure Transformers.

Another exploration of MetaFormer architecture also provided along with the parallel token mixer encoder, we also introduce the Convolutional Attention Patch Embedding (CAPE). The CAPE provide the enhancement of MetaFormer architecture that can enhance the feature learnability even with or without token mixer operator. Through the Channel Attention module, the feature map is selectively highlighted while doing the downsizing in the Patch Embedding

module. Using the CAPE also can enhance the token mixer since the feature is highlighted in early.

## 2 Related Works

**Vision Transformers.** The integration of transformers from natural language processing (NLP) into the field of computer vision was first proposed by [15]. Since then, this idea has garnered considerable attention and has been used to various activities within the domain. Numerous transformer topology have been proposed [30, 31, 45, 46] with the aim of enhancing precision and effectiveness in diverse applications. Generally, these techniques prioritize the attention mechanism of the transformer architecture due to its computational complexity and lack of continuity being identified as the primary challenge. For example, the Pyramid Vision Transformer (PVT) [45] introduced a modification known as Spatial Reduction Attention (SRA), which replaces the Vanilla Attention mechanism. SRA achieves a reduction in computational complexity by employing key and value reductions, while still preserving the global receptive field characteristic of the ViT. On the other hand, the transformer model exhibits a deficiency in terms of local continuity. To address this issue, alternative local approaches, such as the Swin Transformer [31], adopt a strategy of using non-overlapping windows. These windows are gradually shifted to increase the receptive field, thereby capturing interactions across several phases. Therefore, the self-attention mechanism has constraints in its ability to efficiently capture information that spans across great distances.

**Local and Global Dependencies.** In numerous works, the attention-based model transformer is combined with a convolution network or another type of attention model in order to reduce computational complexity and address the issue of discontinuity [4, 9, 12, 16, 18, 28, 33, 51]. In a general context, the process of combining or hybridising can be categorised into two distinct groups: serial combination and parallel combination. Within the framework of a sequential methodology, the integration of the attention module and convolution can yield a serial design [4, 12, 33]. In the initial phase of its architecture, the convolution network performs local field extraction, but in the later stage, it employs the attention module to obtain global receptive capabilities. The purpose of this approach is to ensure that the architecture remains lightweight while still being able to retrieve and store both local and global information. On the other hand, this approach involves implementing parallelism between the local and global extractors within the attention module. The PLG-ViT [16] model exhibits parallelism in its attention mechanisms, specifically in the W-MSA of Swin Transformer as a local extractor and the SRA of PVT as a global extractor. Another approach in Lite Transformer [51], combine vanilla attention as a long range feature capturing with convolution network as local feature capturing in transformer encoder.

**Patch Embedding.** In the initial implementation of the transformer, the image is minimally processed by linear projection, as opposed to the CNN-based model which utilizes convolution with stride in the block to reduce the size of

the image. In the upcoming iteration of Transformer, the vision transformer architecture, which is employed in PVT [45] and CVT [50], incorporates convolution patch embedding. In order to enhance the local coherence, the technique of overlap patch embedding is employed in PVTv2 [46] and CVT [50]. Subsequently, it has been demonstrated that the "patchify" technique may effectively improve the performance of the CNN architecture in ConvNeXt [32]. This enhancement enables the ConvNeXt design to attain comparable results to the Swin Transformer [31]. In our methodology, we draw inspiration from the Squeeze-and-Excitation technique [23] and the Convolutional Block Attention Module (CBAM) [49] to incorporate convolutional attention into the patch embedding process. This is done with the aim of improving the learnability in image patching.

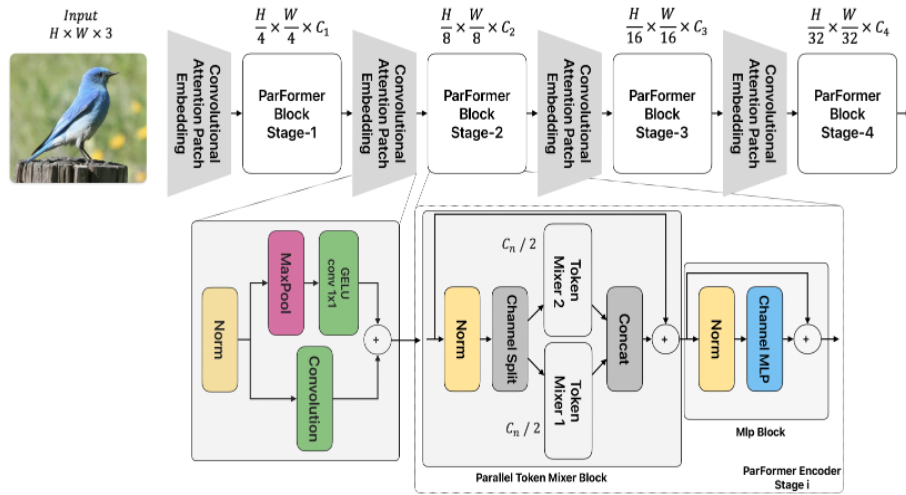


**Fig. 2: The overall ParFormer Framework**, the general architecture that allowed to combine two distinct or similar token mixer. To enhance the feature extraction the token mixer shift is used rather than channel shift [13, 42, 59]. ParFormer used pyramid architecture with 4 stages. The feature dimension is decreased from stride 4 to stride 32 with depth  $[C_1, C_2, C_3, C_4]$ .

## 3 Method

### 3.1 ParFormer

The main idea of ParFormer for this investigation is presented in this part. The ParFormer model incorporates the Convolutional Attention Patch Embedding technique, which enables us to modify the token dimension. This is an improvement over the typical convolutional patch embedding commonly used in current

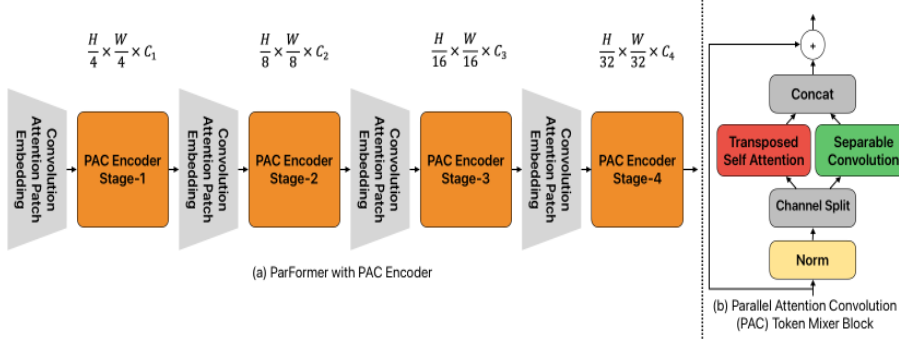


**Fig. 3: The overall ParFormer Framework with Parallel Attention and Convolution Token Mixer for couple the local and global feature**, The future dimension is decreased from stride 4 to stride 32 with channel dimension is increased  $[C_1, C_2, C_3, C_4]$ .

transformer designs. In addition, the channel attention module is employed to augment the feature extraction process by allocating additional attention to specific channels.

**Convolutional Attention Patch Embedding (CAPE).** Convolutional Patch Embedding denotes as the feature summation between the convolutional patch embedding with the Channel Attention Module (CAM) to process the given input image or the feature map  $X_{i-1}$  from the previous stage with the size  $H_{i-1} \times W_{i-1} \times C_{i-1}$  as discribed in Eq. (1).

$$X_i = PatchEmbedding(X_{i-1}) + CAM(X_{i-1}). \quad (1)$$

The input  $X_{i-1}$  will be patched into  $X_i \in \mathbb{R}^{\frac{H_i}{S} \times \frac{W_i}{S} \times C_i}$  with convolution stride  $S$ , kernel size  $2S - 1$ , and padding size  $S - 1$  for the overlapped spatial downsizing and  $C_i$  for the number of feature in the stage- $i$  that can be adjusted.

The Channel Attention Module is derived from Convolutional Block Attention Module (CBAM) [49] and Squeeze-and-Excitation module [23] which can be integrated into the existing model. They have ability to re-calibrate the feature map in each channel such as Squeeze-and-Excitation or in both spatial and channel such as CBAM [49]. In channel attention module, both the CBAM and Squeeze-and-Excitation modules generate descriptors that capture the worldwide distribution of feature responses across channels. This enables all levels of the network to utilize information from the network’s global receptive field.

As depicted in Fig. 4, the global spatial information is captured by MaxPool. Unlike the CBAM or Squeeze-and-Excitation module that global information achieved through the squeeze mechanism with one value in overall spatial, our proposed attention is using overlap MaxPool operation. The purpose of overlap MaxPool with kernel size  $3S - 2$  is to find the most significant information with spatial area more wide than the convolution patch embedding.

$$CAM(X_i) = \sigma(MaxPool(X_i)W_p). \quad (2)$$

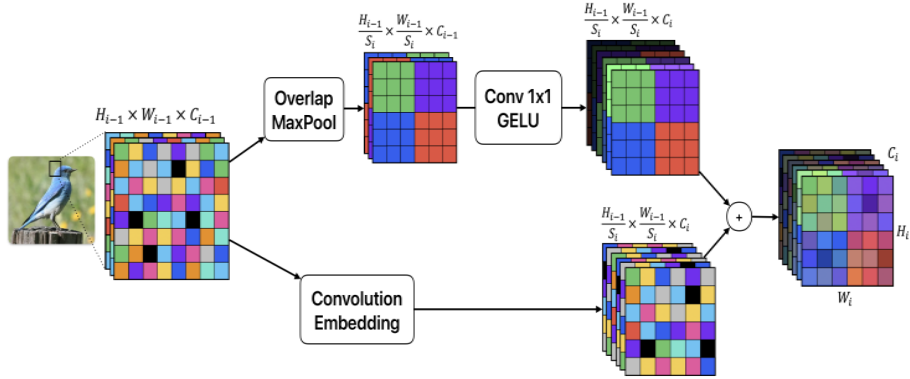


Fig. 4: Convolutional Attention Patch Embedding.

Global information will be subjected to linear operations ( $W_p$ ) to choose the channel to emphasize. The non-linear activation function, denoted as  $\sigma$ , specifically the  $GELU(\cdot)$  function, is used to enable nonlinear learnability. The sum operation is used to combine the spatial learnability of the CAM in the Eq. (2) and the standard convolution patch embedding in order to re-calibrate the feature map.

**Parallel Token Mixer and MLP Block.** The patched image will be incorporated into repeated sequence ParFormer block with two residual sub-block which consist parallel token mixer block and MLP block. The parallel token mixer comprises two token mixers that enable effective extraction of token information by two separate or similar operators. The parallel token mixer is comprised of two token mixers that have been pre-processed utilizing channel splitting in order to divide the tokens across the two mixers. These sub-blocks can be represented in Eq. (6)

$$X_1, X_2 = Split(Norm(X_i)), \quad (3)$$

$$X'_1 = TokenMixer_1(X_1), \quad (4)$$

$$X'_2 = TokenMixer_2(X_2), \quad (5)$$

$$X'_i = X_i + Cat(X'_1, X'_2), \quad (6)$$

where  $X_1, X_2, X'_1, X'_2 \in \mathbb{R}^{\frac{H}{S} \times \frac{W}{S} \times \frac{C'}{2}}$ . The  $Norm(\cdot)$  denotes the Layer Normalization [3] and  $Split(\cdot)$  denotes the the splitting array correspond to channel  $C$ . The  $TokenMixer_1(\cdot)$  and  $TokenMixer_2(\cdot)$  are two different or similar operation module to extract token information such attention [15,16,26] or convolution [43]. The  $Cat(\cdot)$  is the concatenating between  $X'_1$  and  $X'_2$ .

The MLP block employed in this study has resemblance to the original MLP block utilised in the Vision Transformer (ViT) model proposed by Dosovitskiy et al [15]. It encompasses a singular activation function, which may be mathematically represented by the subsequent equation.

$$X''_i = X'_i + (\sigma(Norm(X'_i)W_1))W_2, \quad (7)$$

where  $X', X'' \in \mathbb{R}^{\frac{H}{s} \times \frac{W}{s} \times C'}$ . The  $W_1 \in \mathbb{R}^{C' \times rC'}$  and  $W_2 \in \mathbb{R}^{rC' \times C'}$  are learnable weight with  $r$  MLP expansion ratio. The  $\sigma$  denotes the activation function that can be configured as  $GELU(\cdot)$  [21],  $ReLU(\cdot)$  [1], or another non-linear activation function (*i.e.*  $SiLU(\cdot)$  [17]).

### 3.2 Local and Global Token Mixer in ParFormer Framework

ParFormer is a versatile design that can be modified with various token mixers with the parallel architecture with overall architecture is using common 4-stage model as depicted in Figure 2. Instead of designing the novel token mixer, this study aims to evaluate the ParFormer architecture by testing its performance with two existing different token mixers, such as Attention [15] as global extractor and Convolution token mixer [54] as a local extractor.

In global token mixer, instead used a vanilla attention, the transposed self attention is used [37, 44], since it have lower computational complexity. In transposed self attention, the first step is projected the input  $X$  using linear weight operation  $W_3$  into  $Q$ ,  $K$ , and  $V$  denoted as query, key, and value with  $Q, K, V \in \mathbb{R}^{n \times d}$ , where  $n$  is the number of tokens and  $d$  is the number of attention head dimension.

$$Q, K, V = W_3 * X. \quad (8)$$

Then, find the relationship between each input tokens which can be described as function in Eq. (9). In this operation will reduced the complexity from  $\mathcal{O}(n^2)$  to  $\mathcal{O}(d^2)$ , since the  $Q$  is transposed into  $d^2$  multiplication which the dimension of  $d$  is less than  $n$ .

$$A = softmax(Q^T K). \quad (9)$$

Finally, the output is the relationship matrix  $A$  with the weighted of value  $V$  that obtained from Eq. (10).

$$Attn(X) = VA. \quad (10)$$

For the Convolution token mixer, we follow the inverted bottle neck convolution block from MobileNetV2 [35], but the activation function is in the end of separable convolution block rather than in the early stage [53], as shown in the Eq. (11).

$$X' = Conv_{pw_2}(\sigma(Conv_{dw}(Conv_{pw_1}(X)))), \quad (11)$$

where  $Conv_{pw}(\cdot)$ ,  $Conv_{dw}(\cdot)$  denotes the point-wise convolution and depth-wise convolution. The  $\sigma$  denotes the non-linear activation function. In practical implementation, the kernel size is determined as 7, as suggested by reference [32], and the expansion ratio is set at 2.

### 3.3 Overall Architecture

In the preceding section, we tried to explain the current existing token mixer in the ParFormer approach. This enabled us to assess the efficacy of the model



**Table 1: Model configurations of ParFormer Framework.** “C”, “L” and “T” means channel number, block number and token mixer type. “PAC” denotes token mixer of parallel attention with separable convolution, respectively. The contents in the tuples represent the configurations in the four stages of the models.

Stage	Token Size	Layer Specification		ParFormer		
				B1	B2	B3
Stage-1	$\frac{H}{4} \times \frac{W}{4}$	CAPE	Patch Size	7x7, Stride 4		
			MaxPool	10x10, Stride 4		
			Dim	48	64	96
		ParFormer Encoder	Attn Dim	C=24	C=32	C=48
			Conv Dim	C=24	C=32	C=48
			#Blocks	3	3	3
Stage-2	$\frac{H}{8} \times \frac{W}{8}$	CAPE	Patch Size	3x3, Stride 2		
			MaxPool	4x4, Stride 2		
			Dim	96	128	192
		ParFormer Encoder	Attn Dim	C=48	C=64	C=96
			Conv Dim	C=48	C=64	C=96
			#Blocks	3	3	12
Stage-3	$\frac{H}{16} \times \frac{W}{16}$	CAPE	Patch Size	3x3, Stride 2		
			MaxPool	4x4, Stride 2		
			Dim	192	320	384
		ParFormer Encoder	Attn Dim	C=96	C=160	C=192
			Conv Dim	C=96	C=160	C=192
			#Blocks	9	9	18
Stage-4	$\frac{H}{32} \times \frac{W}{32}$	CAPE	Patch Size	3x3, Stride 2		
			MaxPool	4x4, Stride 2		
			Dim	384	512	768
		ParFormer Encoder	Attn Dim	C=192	C=256	C=384
			Conv Dim	C=192	C=256	C=384
			#Blocks	3	3	3
Classifier Head				Global Pool, Norm, FC		

by employing two comparable token mixers at each level of the encoder. The design of ParFormer as a general-purpose vision transformer utilized four stage pyramid feature maps. The CAPE is used to downsampling the feature with rates 4, 8, 16, 32. For the token mixer, employing two separate token mixers called Parallel Attention Convolution (PAC) token mixer block. The first token mixer utilizes transposed self-attention, while the second token mixer employs separable convolution, such shown in Fig. 3(b). As is often understood, attention mechanisms provide the capability to capture global dependencies, whereas convolutional operations excel in capturing local continuity.

The overall architecture variant of the ParFormer is shown in the Tab. 1. The blocks in each stage and the feature dimension is chosed manually to format a several models in different size, whose the computational complexity ranges

from 1.5G(B1) to 6.5G(B3). The number of block is following the recipe from ConvNeXt [32] and MetaFormer [54].

## 4 Experimental Result

In order to assess the effectiveness of ParFormer, two thorough tests are conducted. The tests involve ImageNet-1K datasets [34] for classification and COCO Datasets [29] for object detection and instance segmentation.

### 4.1 Image Classification

**Preparation.** Image classification experiments are conducted using the ImageNet-1K dataset, consisting of 1.28 million training images and 50,000 validation images across 1,000 categories. Our study used a training recipe similar to those of DeiT [40] and Swin Transformer [31]. The models undergo training for a total of 300 epochs, with a resolution of  $224 \times 224$ . Data augmentation and regularization approaches encompass several methods such as RandAugment [10], Mixup [58], CutMix [57], Random Erasing [60], weight decay, Label Smoothing [24], and Stochastic Depth [39]. The hyper-parameters of DeiT [40] are primarily adhered to in our approach. We employ the AdamW optimizer [52] with 256 batch size on  $2 \times A6000$  GPUs for most ParFormer models. The performance evaluation was conducted without any pre-training on larger datasets like Image-Net21K or at higher resolutions.

**Table 2:** Comparison test of Convolutional Attention Patch Embedding (CAPE) on existing Token Mixer model using ImageNet-1K dataset with  $224 \times 224$  image size.

Model	Patch	Token Mixer	Params	GFLOPs	Top-1
IdentityFormer-S18 [54]	Overlap Conv	Identity	11.9	1.8	74.6
	CAPE	Identity	12.1	1.85	75.0
PVTv2-B1 [46]	Overlap Conv	Hybrid Attn	13.1	2.1	78.8
	CAPE	Hybrid Attn	15.4	2.2	79.5
Swin-T [31]	Hard Patching (C96)	Attn	29	4.5	81.3
	CAPE (C64)	Attn	19	2.7	81.7

**Result of Convolutional Attention Patch Embedding** Initially, we assess the performance of Convolutional Attention Patch Embedding (CAPE) to determine its usefulness without employing a token mixer or utilizing Identity Mapping. In addition, we also assess CAPE on various existent Token Mixers. We assess the Window Multi-head Self Attention (WMSA) of the Swin Transformer

**Table 3:** Comparison of ParFormer with convolution and attention token mixer on ImageNet-1K with 224×224 image size.

Model	Type	Img Size	Params	GFLOPs	Top-1
RSB-ResNet-18 [47]	Conv	224	11	1.8	71.5
ConvNeXt-N [32]	Conv	224	15	2.45	80.8
EfficientViT-M4	Attn	224	12	0.5	77.1
PoolFormer-S12 [53]	Pooling	224	12	1.8	77.2
MixFormer-B2 [8]	Hybrid	224	10	0.9	80.0
PVTv2-B1 [46]	Hybrid	224	13	2.1	78.1
EfficientFormer-L [27]	Hybrid	224	12	1.3	79.3
<b>ParFormer-B1</b>	<b>Hybrid</b>	<b>224</b>	<b>11</b>	<b>1.5</b>	<b>80.4</b>
RSB-ResNet-50 [47]	Conv	224	26	4.1	80.4
ConvNeXt-T [32]	Conv	224	29	4.5	82.1
Swin-T [31]	Attn	224	29	4.5	81.3
CSWin-T [14]	Attn	224	23	4.3	82.3
PLG-ViT-T [16]	Attn	224	27	4.0	82.9
PoolFormer-S24 [53]	Pooling	224	21	3.4	80.2
PVTv2-B2 [46]	Hybrid	224	25	4.0	82.1
CoAtNet-0 [12]	Hybrid	224	25	4.2	81.6
CAFormer-S18 [54]	Hybrid	224	26	4.1	83.6
<b>ParFormer-B2</b>	<b>Hybrid</b>	<b>224</b>	<b>23</b>	<b>3.4</b>	<b>82.1</b>
RSB-ResNet-101 [47]	Conv	224	44	7.9	81.3
ConvNeXt-B [32]	Conv	224	50	8.7	83.0
Swin-B [31]	Attn	224	50	8.7	83.1
CSWin-T [14]	Attn	224	36	6.9	83.6
PLG-ViT-T [16]	Attn	224	35	4.0	82.9
PVTv2-B3 [46]	Hybrid	224	45.	4.0	82.1
MixFormer-B4 [8]	Hybrid	224	35	3.6	83.0
CoAtNet-1 [12]	Hybrid	224	42	8.3	83.3
CAFormer-S36 [54]	Hybrid	224	39	8.0	84.5
<b>ParFormer-B3</b>	<b>Hybrid</b>	<b>224</b>	<b>34</b>	<b>6.5</b>	<b>83.1</b>

model for the Attention Token mixer [31] and the Spatial Reduction Attention (SRA) of PVTv2 for the Hybrid Token Mixer [46].

Tab. 2 demonstrates the capability of CAPE for enhance the performance of MetaFormer like architecture on the ImageNet-1K classification test. By adding 1.7% and 2.7% of Parameters and FLOPs, the CAPE can enhance the accuracy from 74.6 % to 75.0%. This outcome was reached without any fine-tuning using ImageNet-2K pre-training, as typically done in the training step of MetaFormer [54]. Moreover, the ability of CAPE to improve the MetaFormer architecture is evident in the tests conducted with WMSA and SRA Token Mixer. PVTv2’s performance can be improved by about 1% accuracy by adding parameters of up to 20% and increasing FLOPs by 5%. The CAPE has been shown to enhance the performance of the Swin Transformer, which use a pure attention token mixer, even with fewer parameters. Our test with feature channel embedding size starting at 64, as opposed to the original Swin-T which started at 96, achieved

improved accuracy with fewer parameters and computations, addressing the issue of the pure transformer. The qualitative result of CAPE to enhance the token mixer to locate the semantic object can be seen in the Appendix. The test on the ImageNet-1K classification demonstrates that the CAPE can enhance the MetaFormer architecture design, both with the non-parametric token mixer such Identity Mapping and the current token mixer WMSA and SRA.

**Result of ParFormer.** After verifying the capabilities of CAPE, we investigate the token mixer component. We investigate the local and global token mixer by utilizing separable convolution and transposed self-attention in parallel, achieved through separating the channel dimension of the feature map. Tab. 3 shows the ImageNet-1K test results. To ensure a fair comparison, the results are grouped based on the parameter size. The group consists of characteristics ranging from 10 million to 20 million, 20 million to 30 million, and 30 million to 50 million. The table labeled as Tab. 3 demonstrates that The ParFormer can achieve competitive performance with fewer parameters and FLOPs compared to the state-of-the-art models. The ParFormer can reach 80.4% accuracy with fewer parameters (up to 15% less) compared to PVTv2-B1 [46] and EfficientFormer-L [27] which utilizes a hybrid token mixer instead of relying just on pure attention or pure convolution similar to ours. The test indicates that the parallel token mixer utilizing convolution and attention can decrease the parameters and FLOPs demonstrated by ParFormer-B1 and MixFormer-B2 [8]. Our method is unable to outperform MixFormer-B2 [8], which incorporates a channel and spatial interaction module between convolution and attention to serve as a local and global token mixer. This module can enhance the receptive field even in small feature map dimensions ( $C=32$ ), in contrast to ParFormer-B1, which starts with a feature dimension of  $C=48$ . A comparison between models that use hybrid convolution and attention in a sequential design like CoAtNet and CAFormer, and our parallel approach, will be discussed. The ParFormer-B2 and ParFormer-B3 surpass the CoAtNet-0 and CoAtNet-1 [12] models by 8% and 19% in terms of parameters and FLOPs, respectively, when trained without pre-training on the larger ImageNet-21K dataset, compared to the CAFormer-S18 and CAFormer-S36 models. It shows that the parallel approach can achieve the lower parameter and computation while keep maintaining the accuracy.

## 4.2 Ablation Study

In this part, we examine the unique architectural decisions. We offer ablations specifically tailored to our designs on ParFormer-B2. We report all variations of distinct designs on ImageNet-1K [34] classification using the identical hyperparameter as presented in Tab. 3. Below, Tab. 4 shows the ablation based on the following aspects.

**CAPE.** Our initial method, known as Convolutional Attention Patch Embedding (CAPE), distinguishes between the MetaFormer architecture and our own. The comparison between utilizing CAPE and not utilizing CAPE in the MetaFormer architecture, which serves as a universal architecture of the Transformer, has been deliberated. The findings demonstrate that the capacity of

CAPE can improve the structure of MetaFormer [53], as seen by the utilization of the Identity Mapping token mixer. Another method is the utilization of CAPE to improve the performance of attention-based token mixers like WMSA in the Swin Transformer [31]. Utilizing the CAPE technique can enhance accuracy by 0.4%, even while employing a lower feature map dimension of 64, as opposed to the original approach which began embedding the feature with a dimension of 96. This leads to reduced parameters and FLOPs, which can reach up to 40%. Then we evaluate the effect of overlap MaxPool size on the ParFormer-B2 as a baseline, the first step we change the overlap MaxPool kernel size same as the Convolution Patch Embedding that decreasing the accuracy to 82.04 same as the change from overlap maxpool to overlap patch embedding that means the kernel size of convolutional patch embedding larger than MaxPool. Thus we adopt the CAPE with overlap MaxPool.

**Token Mixers.** The upcoming ablation procedure is the parallel token mixer. We aim to investigate the effectiveness of employing a parallel token mixer that combines Pooling, Separable Convolution, and Attention techniques. However, this combination has led to a decrease in accuracy by 4%. However, it is evident that the FLOPs can be decreased by up to 50%. This indicates that the integration of non-parametric and parametric token mixer with parallel architecture can effectively decrease the computational complexity. In addition, we investigate a parallel token mixer that functions as a single-like series token mixer. This mixer combines separable convolution and attention in sequential demonstrations, resulting in a reduction of parameters to 21.2. This reduction is achieved by placing the separable convolution, which has a 2 times expansion ratio, in the early stage. However, it is evident that the accuracy also reduced by 0.2%. Therefore, we choose to utilize the Parallel Separable Convolution and Attention as our token mixer.

**Table 4:** Ablation of Convolutional Attention Patch Embedding (CAPE) with another model tested on ImageNet-1K with  $224 \times 224$  image size.

Ablation	Variant	Params	GFLOPs	Top-1
ParFormer-B2	Baseline	23.2	3.36	82.1
CAPE	Size MaxPool>Conv → MaxPool=Conv	23.2	3.36	82.04
	Size MaxPool>Conv → MaxPool<Conv	23.2	3.36	82.05
	Without Cape	21.2	3.26	81.5
Token Mixer	TM-1=[a, a, a, a] → TM-2=[sc, sc, sc, sc]	15.7	1.7	78.4
	TM-1=[sc, sc, a, a] TM-2=[p, p, p, p]			
	TM-1=[a, a, a, a] → TM-2=[sc, sc, sc, sc]	21.2	3.8	81.9
	TM-1=[sc, sc, a, a] TM-2=[sc, sc, a, a]			

### 4.3 Object Detection and Instance Segmentation

**Preparation.** We assess the efficacy of ParFormer on subsequent assignments. We utilize the Mask R-CNN [19] algorithm to train our method on the COCO2017 train split. Subsequently, we assess the performance of the models on the val split. The training schedule is set at  $1\times$  in order to maintain a consistent comparison with earlier approaches [8, 20, 37, 46]. For the  $1\times$  schedule, we conduct training for 12 epochs using a single size on the  $2\times A6000$  GPUs. AdamW [25] Optimizer is used with initial learning rate is  $2 \times 10^{-2}$  with batch size 16. The training images are scaled to have a shorter side of 800 pixels and a longer side that does not exceed 1,333 pixels. The implementation is derived from the mmdetection [7] code-base. As part of the testing process, the dimension of the images is adjusted to a size of  $1280 \times 800$  pixels.

**Result.** Due to resource constraints, we have chosen to test the ParFormer-B1 model, which has a small size. The ParFormer-B1 model, which incorporates the Mask R-CNN as the object detector, surpasses the ResNet-18 model with a pure convolution backbone. It does this by having 6% and 3.7% smaller parameters and FLOPs, resulting in 4.8 and 4.0 higher box AP and mask AP scores, respectively. Table 5 presents a comparison between the ParFormer-B1 model and the hybrid Token Mixer model. ParFormer-B1 demonstrates superior performance compared to PVT-T, PoolFormer-S12, and EfficientFormer-L1 in terms of box AP for object recognition and mask AP for instance segmentation. Additionally, ParFormer-B1 achieves these results with a 10% reduction in parameters. Nevertheless, the efficacy of the MixFormer-B2’s channel and spatial interaction has been demonstrated to achieve a greater receptive field in object detection and instance segmentation. ParFormer regularly outperforms PVT, PoolFormer, and EfficientFormer in COCO object detection and instance segmentation, demonstrating competitive performance.

**Table 5:** Object detection and instance segmentation on COCO val2017 with Mask R-CNN.  $AP^b$  and  $AP^m$  denote bounding box average precision and mask average precision, respectively. The FLOPs (G) are measured at resolution  $1280 \times 800$ .

Backbone	$AP^b$	$AP_{50}^b$	$AP_{75}^b$	$AP^m$	$AP_{50}^m$	$AP_{75}^m$	Params	FLOPs
ResNet-18 [20]	34.0	54.0	36.7	31.2	51.0	32.7	31.2	207.4G
PVT-T [46]	36.7	59.2	39.3	35.1	56.7	37.3	32.8	239.8G
PVTv2-B1 [46]	41.8	64.3	45.9	38.8	61.2	41.6	33.7	243.7G
PoolFormer-S12 [53]	37.3	59.0	40.1	34.6	55.8	36.9	31.6	207.3G
MixFormer-B2 [8]	41.5	63.3	45.2	38.3	60.6	41.2	28.0	187.0G
EfficientFormer-L1 [27]	37.9	60.3	41.0	35.4	57.3	37.3	31.5	196.4G
<b>ParFormer-B1</b>	<b>39.5</b>	<b>61.2</b>	<b>42.6</b>	<b>36.7</b>	<b>58.3</b>	<b>39.0</b>	<b>29.4</b>	<b>200.0G</b>
ResNet-50 [20]	34.0	54.0	36.7	31.2	51.0	32.7	31.2	207.4G
PVT-S [46]	40.4	62.9	43.8	37.8	60.1	40.3	44.1	304.5G
PVTv2-B2 [46]	44.6	65.6	47.6	27.4	48.8	58.6	45.2	309.2G
PoolFormer-S24 [53]	40.1	62.2	43.4	37.0	59.1	39.6	41.0	239.7G
<b>ParFormer-B2</b>	<b>42.1</b>	<b>64.4</b>	<b>45.8</b>	<b>38.6</b>	<b>61.4</b>	<b>40.9</b>	<b>40.3</b>	<b>237.6G</b>

## 5 Conclusion

This work proposes the improvement of the overall Transformer design by including Convolutional Attention Patch Embedding (CAPE), which enhances feature extraction during the patching process. The ParFormer architecture, also known as the Parallel Token Mixer, proposes the integration of two different Token Mixers: Separable Convolution and Transposed Self Attention. This integration enables the extraction of both local and global dependencies. The aim of this study is to showcase the effectiveness of Convolution Attention Patch Embedding and the parallel token mixer architecture through the integration of traditional convolution block and attention-based token mixer. The CAPE showcases its potential to improve the overall architecture of transformers through image patching with a slight increase in parameter and computation. The efficacy of the parallel token Mixer, which enables the fusion of local convolution and global attention token mixer, has been demonstrated through image classification and downstream vision tests. It has shown superior performance compared to a pure convolution and transformer model, while utilizing the fewest parameters and computational resources. The designs in ParFormer are anticipated to function as a foundational framework for creating networks that are highly efficient.

## References

1. Agarap, A.F.: Deep learning using rectified linear units (relu). arXiv preprint arXiv:1803.08375 (2018)
2. Arnab, A., Dehghani, M., Heigold, G., Sun, C., Lučić, M., Schmid, C.: Vivit: A video vision transformer. In: Proceedings of the IEEE/CVF international conference on computer vision. pp. 6836–6846 (2021)
3. Ba, J.L., Kiros, J.R., Hinton, G.E.: Layer normalization. arXiv preprint arXiv:1607.06450 (2016)
4. Cai, H., Gan, C., Han, S.: Efficientvit: Enhanced linear attention for high-resolution low-computation visual recognition. arXiv preprint arXiv:2205.14756 (2022)
5. Carion, N., Massa, F., Synnaeve, G., Usunier, N., Kirillov, A., Zagoruyko, S.: End-to-end object detection with transformers. In: European conference on computer vision. pp. 213–229. Springer (2020)
6. Chen, C.F., Panda, R., Fan, Q.: Regionvit: Regional-to-local attention for vision transformers. arXiv preprint arXiv:2106.02689 (2021)
7. Chen, K., Wang, J., Pang, J., Cao, Y., Xiong, Y., Li, X., Sun, S., Feng, W., Liu, Z., Xu, J., et al.: Mmdetection: Open mmlab detection toolbox and benchmark. arXiv preprint arXiv:1906.07155 (2019)
8. Chen, Q., Wu, Q., Wang, J., Hu, Q., Hu, T., Ding, E., Cheng, J., Wang, J.: Mixerformer: Mixing features across windows and dimensions. In: Proceedings of the IEEE/CVF conference on computer vision and pattern recognition. pp. 5249–5259 (2022)
9. Chu, X., Tian, Z., Wang, Y., Zhang, B., Ren, H., Wei, X., Xia, H., Shen, C.: Twins: Revisiting the design of spatial attention in vision transformers. *Advances in Neural Information Processing Systems* **34**, 9355–9366 (2021)

10. Cubuk, E.D., Zoph, B., Shlens, J., Le, Q.V.: Randaugment: Practical automated data augmentation with a reduced search space. In: Proceedings of the IEEE/CVF conference on computer vision and pattern recognition workshops. pp. 702–703 (2020)
11. Dai, Z., Cai, B., Lin, Y., Chen, J.: Up-detr: Unsupervised pre-training for object detection with transformers. In: Proceedings of the IEEE/CVF conference on computer vision and pattern recognition. pp. 1601–1610 (2021)
12. Dai, Z., Liu, H., Le, Q.V., Tan, M.: Coatnet: Marrying convolution and attention for all data sizes. *Advances in neural information processing systems* **34**, 3965–3977 (2021)
13. Deng, S.Q., Deng, L.J., Wu, X., Ran, R., Hong, D., Vivone, G.: Psrt: Pyramid shuffle-and-reshuffle transformer for multispectral and hyperspectral image fusion. *IEEE Transactions on Geoscience and Remote Sensing* **61**, 1–15 (2023)
14. Dong, X., Bao, J., Chen, D., Zhang, W., Yu, N., Yuan, L., Chen, D., Guo, B.: Cswin transformer: A general vision transformer backbone with cross-shaped windows. In: Proceedings of the IEEE/CVF Conference on Computer Vision and Pattern Recognition. pp. 12124–12134 (2022)
15. Dosovitskiy, A., Beyer, L., Kolesnikov, A., Weissenborn, D., Zhai, X., Unterthiner, T., Dehghani, M., Minderer, M., Heigold, G., Gelly, S., et al.: An image is worth 16x16 words: Transformers for image recognition at scale. arXiv preprint arXiv:2010.11929 (2020)
16. Ebert, N., Stricker, D., Wasenmüller, O.: Plg-vit: Vision transformer with parallel local and global self-attention. *Sensors* **23**(7), 3447 (2023)
17. Elfving, S., Uchibe, E., Doya, K.: Sigmoid-weighted linear units for neural network function approximation in reinforcement learning. *Neural networks* **107**, 3–11 (2018)
18. Guo, J., Han, K., Wu, H., Tang, Y., Chen, X., Wang, Y., Xu, C.: Cmt: Convolutional neural networks meet vision transformers. In: Proceedings of the IEEE/CVF Conference on Computer Vision and Pattern Recognition. pp. 12175–12185 (2022)
19. He, K., Gkioxari, G., Dollár, P., Girshick, R.: Mask r-cnn. In: Proceedings of the IEEE international conference on computer vision. pp. 2961–2969 (2017)
20. He, K., Zhang, X., Ren, S., Sun, J.: Deep residual learning for image recognition. In: Proceedings of the IEEE conference on computer vision and pattern recognition. pp. 770–778 (2016)
21. Hendrycks, D., Gimpel, K.: Gaussian error linear units (gelus). arXiv preprint arXiv:1606.08415 (2016)
22. Hou, Q., Lu, C.Z., Cheng, M.M., Feng, J.: Conv2former: A simple transformer-style convnet for visual recognition. arXiv preprint arXiv:2211.11943 (2022)
23. Hu, J., Shen, L., Sun, G.: Squeeze-and-excitation networks. In: Proceedings of the IEEE conference on computer vision and pattern recognition. pp. 7132–7141 (2018)
24. Huang, G., Liu, Z., Van Der Maaten, L., Weinberger, K.Q.: Densely connected convolutional networks. In: Proceedings of the IEEE conference on computer vision and pattern recognition. pp. 4700–4708 (2017)
25. Kingma, D.P., Ba, J.: Adam: A method for stochastic optimization. arXiv preprint arXiv:1412.6980 (2014)
26. Li, J., Yan, Y., Liao, S., Yang, X., Shao, L.: Local-to-global self-attention in vision transformers. arXiv preprint arXiv:2107.04735 (2021)
27. Li, Y., Yuan, G., Wen, Y., Hu, J., Evangelidis, G., Tulyakov, S., Wang, Y., Ren, J.: Efficientformer: Vision transformers at mobilenet speed. *Advances in Neural Information Processing Systems* **35**, 12934–12949 (2022)



28. Li, Y., Zhang, K., Cao, J., Timofte, R., Van Gool, L.: Localvit: Bringing locality to vision transformers. arXiv preprint arXiv:2104.05707 (2021)
29. Lin, T.Y., Maire, M., Belongie, S., Hays, J., Perona, P., Ramanan, D., Dollár, P., Zitnick, C.L.: Microsoft coco: Common objects in context. In: Computer Vision–ECCV 2014: 13th European Conference, Zurich, Switzerland, September 6–12, 2014, Proceedings, Part V 13. pp. 740–755. Springer (2014)
30. Liu, Z., Hu, H., Lin, Y., Yao, Z., Xie, Z., Wei, Y., Ning, J., Cao, Y., Zhang, Z., Dong, L., et al.: Swin transformer v2: Scaling up capacity and resolution. In: Proceedings of the IEEE/CVF conference on computer vision and pattern recognition. pp. 12009–12019 (2022)
31. Liu, Z., Lin, Y., Cao, Y., Hu, H., Wei, Y., Zhang, Z., Lin, S., Guo, B.: Swin transformer: Hierarchical vision transformer using shifted windows. In: Proceedings of the IEEE/CVF international conference on computer vision. pp. 10012–10022 (2021)
32. Liu, Z., Mao, H., Wu, C.Y., Feichtenhofer, C., Darrell, T., Xie, S.: A convnet for the 2020s. In: Proceedings of the IEEE/CVF conference on computer vision and pattern recognition. pp. 11976–11986 (2022)
33. Mehta, S., Rastegari, M.: Mobilevit: light-weight, general-purpose, and mobile-friendly vision transformer. arXiv preprint arXiv:2110.02178 (2021)
34. Russakovsky, O., Deng, J., Su, H., Krause, J., Satheesh, S., Ma, S., Huang, Z., Karpathy, A., Khosla, A., Bernstein, M., et al.: Imagenet large scale visual recognition challenge. *International journal of computer vision* **115**, 211–252 (2015)
35. Sandler, M., Howard, A., Zhu, M., Zhmoginov, A., Chen, L.C.: Mobilenetv2: Inverted residuals and linear bottlenecks. In: Proceedings of the IEEE conference on computer vision and pattern recognition. pp. 4510–4520 (2018)
36. Selvaraju, R.R., Cogswell, M., Das, A., Vedantam, R., Parikh, D., Batra, D.: Grad-cam: Visual explanations from deep networks via gradient-based localization. In: Proceedings of the IEEE international conference on computer vision. pp. 618–626 (2017)
37. Shen, Z., Zhang, M., Zhao, H., Yi, S., Li, H.: Efficient attention: Attention with linear complexities. In: Proceedings of the IEEE/CVF winter conference on applications of computer vision. pp. 3531–3539 (2021)
38. Strudel, R., Garcia, R., Laptev, I., Schmid, C.: Segmenter: Transformer for semantic segmentation. In: Proceedings of the IEEE/CVF international conference on computer vision. pp. 7262–7272 (2021)
39. Szegedy, C., Vanhoucke, V., Ioffe, S., Shlens, J., Wojna, Z.: Rethinking the inception architecture for computer vision. In: Proceedings of the IEEE conference on computer vision and pattern recognition. pp. 2818–2826 (2016)
40. Touvron, H., Cord, M., Douze, M., Massa, F., Sablayrolles, A., Jégou, H.: Training data-efficient image transformers & distillation through attention. In: International conference on machine learning. pp. 10347–10357. PMLR (2021)
41. Vaswani, A., Shazeer, N., Parmar, N., Uszkoreit, J., Jones, L., Gomez, A.N., Kaiser, Ł., Polosukhin, I.: Attention is all you need. *Advances in neural information processing systems* **30** (2017)
42. Wang, G., Zhao, Y., Tang, C., Luo, C., Zeng, W.: When shift operation meets vision transformer: An extremely simple alternative to attention mechanism. In: Proceedings of the AAAI Conference on Artificial Intelligence. vol. 36, pp. 2423–2430 (2022)
43. Wang, J., Yin, P., Wang, Y., Yang, W.: Cmat: Integrating convolution mixer and self-attention for visual tracking. *IEEE Transactions on Multimedia* (2023)

44. Wang, S., Li, B.Z., Khabsa, M., Fang, H., Ma, H.: Linformer: Self-attention with linear complexity. arXiv preprint arXiv:2006.04768 (2020)
45. Wang, W., Xie, E., Li, X., Fan, D.P., Song, K., Liang, D., Lu, T., Luo, P., Shao, L.: Pyramid vision transformer: A versatile backbone for dense prediction without convolutions. In: Proceedings of the IEEE/CVF international conference on computer vision. pp. 568–578 (2021)
46. Wang, W., Xie, E., Li, X., Fan, D.P., Song, K., Liang, D., Lu, T., Luo, P., Shao, L.: Pvt v2: Improved baselines with pyramid vision transformer. Computational Visual Media **8**(3), 415–424 (2022)
47. Wightman, R., Touvron, H., Jégou, H.: Resnet strikes back: An improved training procedure in timm. arXiv preprint arXiv:2110.00476 (2021)
48. Woo, S., Debnath, S., Hu, R., Chen, X., Liu, Z., Kweon, I.S., Xie, S.: Convnext v2: Co-designing and scaling convnets with masked autoencoders. In: Proceedings of the IEEE/CVF Conference on Computer Vision and Pattern Recognition. pp. 16133–16142 (2023)
49. Woo, S., Park, J., Lee, J.Y., Kweon, I.S.: Cbam: Convolutional block attention module. In: Proceedings of the European conference on computer vision (ECCV). pp. 3–19 (2018)
50. Wu, H., Xiao, B., Codella, N., Liu, M., Dai, X., Yuan, L., Zhang, L.: Cvt: Introducing convolutions to vision transformers. In: Proceedings of the IEEE/CVF international conference on computer vision. pp. 22–31 (2021)
51. Wu, Z., Liu, Z., Lin, J., Lin, Y., Han, S.: Lite transformer with long-short range attention. arXiv preprint arXiv:2004.11886 (2020)
52. You, Y., Li, J., Reddi, S., Hseu, J., Kumar, S., Bhojanapalli, S., Song, X., Demmel, J., Keutzer, K., Hsieh, C.J.: Large batch optimization for deep learning: Training bert in 76 minutes. arXiv preprint arXiv:1904.00962 (2019)
53. Yu, W., Luo, M., Zhou, P., Si, C., Zhou, Y., Wang, X., Feng, J., Yan, S.: Metaformer is actually what you need for vision. In: Proceedings of the IEEE/CVF conference on computer vision and pattern recognition. pp. 10819–10829 (2022)
54. Yu, W., Si, C., Zhou, P., Luo, M., Zhou, Y., Feng, J., Yan, S., Wang, X.: Metaformer baselines for vision. IEEE Transactions on Pattern Analysis and Machine Intelligence pp. 1–17 (2023). <https://doi.org/10.1109/TPAMI.2023.3329173>
55. Yu, W., Zhou, P., Yan, S., Wang, X.: Inceptionnext: When inception meets convnext. arXiv preprint arXiv:2303.16900 (2023)
56. Yuan, L., Chen, Y., Wang, T., Yu, W., Shi, Y., Jiang, Z.H., Tay, F.E., Feng, J., Yan, S.: Tokens-to-token vit: Training vision transformers from scratch on imagenet. In: Proceedings of the IEEE/CVF international conference on computer vision. pp. 558–567 (2021)
57. Yun, S., Han, D., Oh, S.J., Chun, S., Choe, J., Yoo, Y.: Cutmix: Regularization strategy to train strong classifiers with localizable features. In: Proceedings of the IEEE/CVF international conference on computer vision. pp. 6023–6032 (2019)
58. Zhang, H., Cisse, M., Dauphin, Y.N., Lopez-Paz, D.: mixup: Beyond empirical risk minimization. arXiv preprint arXiv:1710.09412 (2017)
59. Zhang, X., Zhou, X., Lin, M., Sun, J.: Shufflenet: An extremely efficient convolutional neural network for mobile devices. In: Proceedings of the IEEE conference on computer vision and pattern recognition. pp. 6848–6856 (2018)
60. Zhong, Z., Zheng, L., Kang, G., Li, S., Yang, Y.: Random erasing data augmentation. In: Proceedings of the AAAI conference on artificial intelligence. vol. 34, pp. 13001–13008 (2020)

## Supplementary Material

### A Detailed Experimental Setting

#### A.1 Image Classification

The image classification tests are conducted using the most popular ImageNet-1K dataset for fair comparison between ParFormer and the related model on the state-of-the-art. The ImageNet-1K dataset consist 1.28 million training images and 50,000 validation images across 1,000 categories. The ParFormer image classification test conducted using the regular training on ImageNet-1K without any pre-training on the larger dataset such as ImageNet-22K. The training setting mostly following [32]. However, due to the instability using high learning rate during the training, then we reduce the number of learning and apply different learning rate in each model. The detail of hyper-parameter is described in the Tab. 6. The finetune process done using 224<sup>2</sup> using ImageNet-1K. We consider to finetune on the same dataset using lower learning rate from the pre-train to know the limitation of model in each size. We adopt LAMB optimizer during the finetune since it provide high stability.

**Table 6:** Hyper-parameter of ParFormer for Image Classifications on ImageNet-1K

Hyper-parameter	ParFormer-B1/B2		ParFormer-B3	
	Train	Finetune	Train	Finetune
Optimizer	AdamW	LAMB	AdamW	LAMB
Epoch	300	30	300	30
Base lr	$1.5e^{-3}$	$1e^{-4}$	$1e^{-3}$	$1e^{-4}$
Batch size	256	128	256	128
Weight decay	0.05	$1.8e^{-5}$	0.05	$1.8e^{-5}$
Resolution	224 <sup>2</sup>	224 <sup>2</sup>	224 <sup>2</sup>	224 <sup>2</sup>
lr Scheduler	cosine decay		cosine decay	
Warmup epoch	20	None	20	None
Warmup scheduler	Linear	None	Linear	None
randaugment	(9, 0.5)		(9, 0.5)	
mixup	0.8	None	0.8	None
cutmix	1.0	None	1.0	None
random erasing	0.25		0.25	
label smoothing	0.1		0.1	
stochastic depth	0.1/0.1		0.15	
layer scale	$1e^{-6}$	pre-trained	$1e^{-6}$	pre-trained
head init scale	None	0.001	None	0.001
gradient clip	None	None	None	None
EMA	0.9999	None	0.9999	None

## A.2 Object Detection and Instance Segmentation

COCO 2017 [29] is selected to test the ParFormer in downstream vision task such as object detection and instance segmentation. COCO [29] is selected since it is widely-used large-scale object detection and instance segmentation dataset. Coco 2017 contain 118K images for training and 5K images for validation.

The object detection and instance segmentation test conducted with Mask R-CNN as a frame work and ParFormer as the backbone using mmdet [7]. We employ AdamW optimizer [25] with learning rate  $1e^{-5}$  weight decay of 0.05, batch size of 16 on  $1\times$  schedule of training with 12 epoch. We also extend the object detection test on ParFormer-B2 that shows in Tab. 7

**Table 7:** Object detection and instance segmentation on COCO val2017 with Mask R-CNN.  $AP^b$  and  $AP^m$  denote bounding box average precision and mask average precision, respectively. The FLOPs (G) are measured at resolution  $1280 \times 800$ .

Backbone	$AP^b$	$AP_{50}^b$	$AP_{75}^b$	$AP^m$	$AP_{50}^m$	$AP_{75}^m$	Params	FLOPs
ResNet-18 [20]	34.0	54.0	36.7	31.2	51.0	32.7	31.2	207.4G
PVT-T [46]	36.7	59.2	39.3	35.1	56.7	37.3	32.8	239.8G
PVTv2-B1 [46]	41.8	64.3	45.9	38.8	61.2	41.6	33.7	243.7G
PoolFormer-S12 [53]	37.3	59.0	40.1	34.6	55.8	36.9	31.6	207.3G
MixFormer-B2 [8]	41.5	63.3	45.2	38.3	60.6	41.2	28.0	187.0G
EfficientFormer-L1 [27]	37.9	60.3	41.0	35.4	57.3	37.3	31.5	196.4G
<b>ParFormer-B1</b>	<b>38.8</b>	<b>61.8</b>	<b>41.5</b>	<b>36.2</b>	<b>58.5</b>	<b>38.5</b>	<b>29.4</b>	<b>200.0G</b>
ResNet-50 [20]	34.0	54.0	36.7	31.2	51.0	32.7	31.2	207.4G
PVT-S [46]	40.4	62.9	43.8	37.8	60.1	40.3	44.1	304.5G
PVTv2-B2 [46]	44.6	65.6	47.6	27.4	48.8	58.6	45.2	309.2G
PoolFormer-S24 [53]	40.1	62.2	43.4	37.0	59.1	39.6	41.0	239.7G
<b>ParFormer-B2</b>	<b>42.1</b>	<b>64.4</b>	<b>45.8</b>	<b>38.6</b>	<b>61.4</b>	<b>40.9</b>	<b>40.3</b>	<b>237.6G</b>

## B Qualitative Result

### B.1 Image Classification

We use Grad-CAM [36] to visualize the results of different models trained on ImageNet-1K. We found from Fig. 5 that our PACFormer can segmented the specific object such as screw driver compare to others. For more general our approach result more similar to [54] that combine the attention base and convolutional base token mixer. Our approach result is different compare to the ConvNeXt [32] with more spread in spatial.

### B.2 Object Detection and Instance Segmentation

In Fig. 6, we also visualize some qualitative object detection and instance segmentation results on COCO2017 [29]. These results demonstrate that ParFormer

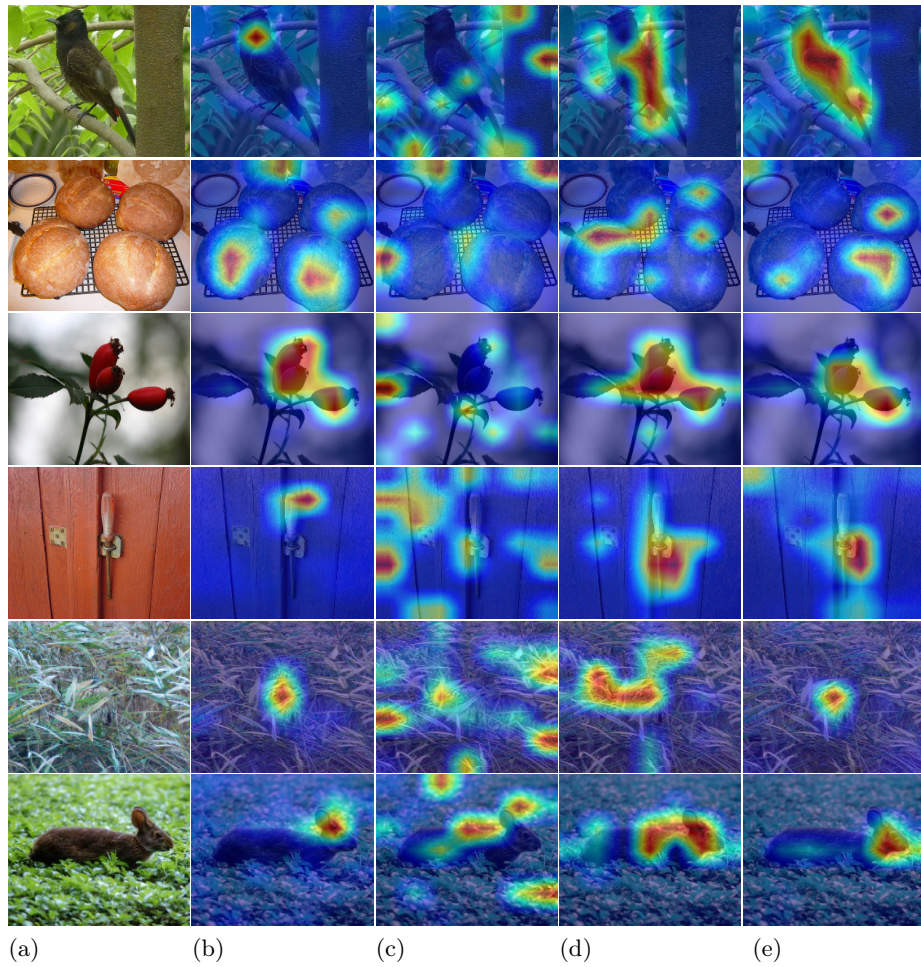


**Fig. 5:** Grad-CAM [36] comparison of (b)ParFormer (c) ConvNeXt [32] (d)Swin-Transformer [31] (e)CAFormer [54] with input (a) with image resolution  $224^2$

backbones can extract powerful features for object detection and instance segmentation, benefiting from the CAPE and parallel attention and convolution architecture designs.



**Fig. 6:** Qualitative results of object detection and instance segmentation on COCO test2017 [29]